





Inertial rotational diffusion and magnetic relaxation of the spin system in a strong magnetic fieldSergei V. Titov ^{1,*}, William J. Dowling ², Vasilii A. Shchelkonogov ^{1,3} and Anton S. Titov ⁴¹*Kotel'nikov Institute of Radio Engineering and Electronics of the Russian Academy of Sciences, Fryazino, Moscow Region 141190, Russia*²*Department of Electronic and Electrical Engineering, Trinity College Dublin, Dublin 2, Ireland*³*Pirogov Russian National Research Medical University, Ostrovityanova st., Moscow 117997, Russia*⁴*The Moscow Institute of Physics and Technology (State University), Institutskiy per. 9, Dolgoprudny, Moscow Region 141701, Russia*

(Received 20 February 2023; revised 29 April 2023; accepted 8 May 2023; published 17 May 2023)

Analytical expressions for the longitudinal and transverse correlation functions pertaining to inertial magnetic relaxation are obtained by expanding the deterministic magnetization trajectories into a Fourier series and averaging the result over all possible initial conditions applying the stationary Boltzmann distribution function. The longitudinal and transverse components of the magnetic susceptibility tensor are calculated for a system of noninteracting macrospins in a strong uniform external field using Bloch's phenomenological approach, which postulates the exponential evolution of the spin system towards equilibrium, and the Lorentz model of rotational diffusion of the magnetization vector. It is shown that the strength of the external field and the magnitude of the inertia parameters noticeably affect the shape of the susceptibility in the THz (nutational resonance) spectrum region. It is also demonstrated that the simple analytical Lorentz-type expression describes the main features of the complex susceptibility in the ferromagnetic resonance and nutation resonance regions.

DOI: [10.1103/PhysRevB.107.174426](https://doi.org/10.1103/PhysRevB.107.174426)**I. INTRODUCTION**

The study of the inertial dynamics of magnetization in nanomagnets and the associated nutational resonance (NR) has attracted great interest in recent years [1–13]. Recently, experimental evidence for inertial dynamics of magnetization in nanoscale ferromagnets, as manifested by magnetization nutation analogous to that usually associated with a symmetric spinning top, has been reported [1]. The nutation resonance of forced oscillations in ferromagnetic thin films occurs at ultrahigh frequencies, of the order of 0.5 THz, and is well separated from the ferromagnetic resonance (FMR), which usually lies in the GHz region. The phenomenon of ultrahigh frequency magnetization nutation is likely to be of some importance for ultrafast manipulation of the magnetic order, which is currently one of the most investigated topics in spintronics [2–4]. Various physical models have been proposed to justify the inertial behavior of the magnetization [5–10,14–17]. A variety of theoretical models make it possible to study more widely the nutation dynamics of magnetization and its role in various magnetic phenomena. These studies are important not only from a fundamental point of view, but are also of practical significance, as terahertz frequencies at which nutation is manifested are important for technological applications.

It was found that theoretically nutation can be described by including an additional term in the Landau-Lifshitz-Gilbert (LLG) equation, which contains the second order derivative of the magnetization \mathbf{M} with respect to time [5–8,12]. The inertial term in the inertial Landau-Lifshitz-Gilbert (ILLG) equation thus obtained is significant over the ultrafast time

scale of subpicoseconds and shorter [1] and accounts for ultrahigh frequency longitudinal and transverse oscillations of the magnetization due to nutation. In coexistence with damping, this nutation disappears in a short time [5]. Despite the novel experimental evidence, and the significant theoretical progress in understanding the microscopic origin of inertia [18–27], inertial relaxation in spin systems affected by thermal noise has not been adequately studied [21,28]. However, under normal environmental conditions, due to the small size of ferromagnetic particles (~ 10 nm), thermal fluctuations caused by thermal noise play a significant role.

The ILLG equation ignores the thermal fluctuations arising because the nanomagnet is maintained at a finite temperature T . If these fluctuations are included, the precessional motion would endure due to the energy provided by the heat bath. The theory of the thermal fluctuations of the magnetization, having been initiated by Néel [29,30], was further developed by Brown [31,32] who set it in the context of the general theory of stochastic processes. To include thermal fluctuations, Brown [31] in 1963 simply added a random isotropic noise magnetic field \mathbf{h} to the LLG equation, which in direct contrast to the dissipative field acts as a source of energy to the system. The same idea was realized in Ref. [21], where the random magnetic field \mathbf{h} was added to the ILLG equation. The resulting generalized nonlinear vector magnetic Langevin equation is written as [21]

$$\frac{d\mathbf{M}}{dt} = \mathbf{M} \times \left(-\gamma(\mathbf{H}_{\text{eff}} + \mathbf{h}) + \frac{\alpha}{M_S} \frac{d\mathbf{M}}{dt} + \frac{\tau}{M_S} \frac{d^2\mathbf{M}}{dt^2} \right), \quad (1)$$

where $\gamma = 2.2 \times 10^5 \text{ rad m A}^{-1} \text{ s}^{-1}$ is the gyromagnetic ratio, M_S is the saturation magnetization, $\mathbf{H}_{\text{eff}} = \mathbf{H} + \mathbf{H}_a(\mathbf{M})$ is the effective magnetic field, including internal anisotropic $\mathbf{H}_a(\mathbf{M})$ and external applied \mathbf{H} magnetic fields, α is the Gilbert precession damping parameter, and τ is the inertial parameter.

*pashkin1212@yandex.ru

The random magnetic field \mathbf{h} is regarded as spatially isotropic Gaussian white noise [21,33]. The magnetic Langevin equation can be used to treat stochastic magnetization dynamics. For example, it makes it possible to describe the reversal of the magnetization (unwanted in magnetic recording) from one metastable state to another due to thermal fluctuations. The magnetic Langevin equation, Eq. (1), ultimately determines the magnetic Fokker-Planck equation for the distribution function of the coordinates of vector \mathbf{M} in the phase space [5,21]. The stationary solution of this Fokker-Planck equation facilitates the calculation of the equilibrium correlation functions of the magnetization [28].

Here, to investigate the inertial magnetic relaxation of spin ensembles in a strong magnetic field including thermal agitation, we derive *analytical* expressions for the time-dependent equilibrium longitudinal and transverse correlation functions of the magnetization. The general solution of the inertial Landau-Lifshitz-Gilbert Eq. (1) is a rather complicated problem due to the need to take into account the magnetocrystalline anisotropy of ferromagnetic particles [22]. The problem significantly simplifies and becomes universal (the form of the magnetocrystalline anisotropy is no longer important) if the contribution of the internal anisotropic field can be neglected in comparison with a strong external magnetic field, $|\mathbf{H}_a(\mathbf{M})| \ll |\mathbf{H}|$. This approximation makes it possible to obtain *analytical* expressions for the components of the susceptibility tensor of the spin system, valid *in the presence of the thermal agitation*. Moreover, some other spin systems with no magnetocrystalline anisotropy can be considered in the same way, for example, electrons under the action of an external field, embedded in a dense medium, which may be either liquid or solid, so that the spins are coupled to all the other degrees of freedom, traditionally called “the lattice” by reference to the crystalline lattice of solids. The temporal correlation functions are used for the description of the temporal evolution of microscopic variables, such as the components of magnetization of ferromagnetic nanoparticles, and its influence on the value of the same microscopic variables at a later time. These correlations are important in equilibrium systems, because a time-invariant macroscopic ensemble can still have nontrivial temporal dynamics microscopically. Moreover, according to linear response theory, there is a relationship between the equilibrium correlation function and the susceptibility [34]. Thus, the longitudinal and transverse components of the magnetic susceptibility tensor are also calculated for a system of noninteracting macrospins in a strong uniform external field.

II. EQUILIBRIUM LONGITUDINAL CORRELATION FUNCTION

The derivation of correlation functions is based on averaging deterministic trajectories $\mathbf{M}(t)$ over all possible initial conditions $\vartheta_0 = \vartheta(0)$, $\varphi_0 = \varphi(0)$, $\omega_x^0 = \dot{\vartheta}(0)$, and $\omega_y^0 = \dot{\varphi}(0) \sin \vartheta(0)$, using a stationary distribution function $W_{st}(\vartheta_0, \varphi_0, \omega_x^0, \omega_y^0)$. Here ϑ and φ are the polar and azimuthal angles of the spherical polar coordinate system determining the direction of vector $\mathbf{M}(t)$ [22,35,36]. Expressions for deterministic trajectories of motion of the magnetization of ferromagnetic nanoparticles can be obtained by solving

Eq. (1) with $\alpha = 0$ and $\mathbf{h} = 0$. These expressions are rather complicated and contain the Jacobi elliptic functions and elliptic integrals [22]. Simplification of the problem is achieved, when the external magnetic field applied along the Z axis $\mathbf{H} = H\mathbf{e}_Z$ is much larger than the internal anisotropic one, $\mathbf{H}_a(\mathbf{M})$, and the internal field can be neglected [35]. Equation (1) can be rewritten as an equation for the unit vector $\mathbf{u} = \mathbf{M}/M_S$, directed along the magnetization vector, which with negligible α , \mathbf{h} , and $\mathbf{H}_a(\mathbf{M})$ has the form

$$\dot{\mathbf{u}} = \gamma[\mathbf{H} \times \mathbf{u}] + \tau[\mathbf{u} \times \ddot{\mathbf{u}}]. \quad (2)$$

It should be noted that in strong external fields a ferromagnet is close to saturation, and therefore the solution of Eq. (2) can be sought by the perturbation method as a correction $\Delta\mathbf{M}(t) = M_S\Delta\mathbf{u}(t)$ to the saturation state $\mathbf{M}_0 \approx M_S\mathbf{e}_Z$, namely $\mathbf{M} = M_S\mathbf{e}_Z + M_S\Delta\mathbf{u}(t)$ [37]. However, such solutions violate the principle of invariability of the magnitude of the magnetization vector $|\mathbf{M}(t)| = M_S$ [22]. Moreover, it is not possible to use perturbed trajectories to calculate the correlation functions of magnetization, where averaging over all possible initial conditions is required, including those violating the condition $\Delta\mathbf{M}(t) \ll \mathbf{M}_0$. The solution of Eq. (2) is briefly described in Appendix A (see also [22,35]).

Having determined the longitudinal $u_{\parallel}(t) = \cos \vartheta(t)$ (along the Z axis) and transverse (perpendicular to the Z axis) components $u_{\perp}(t) = \sin \vartheta(t) \cos \varphi(t)$ of vector \mathbf{u} we can now calculate the longitudinal $C_{\parallel}^{un}(t) = \langle u_{\parallel}(0)u_{\parallel}(t) \rangle - \langle u_{\parallel}(0) \rangle^2$ and transverse $C_{\perp}^{un}(t) = \langle u_{\perp}(0)u_{\perp}(t) \rangle$ equilibrium correlation functions of the undamped rotation of magnetization. The equilibrium ensemble averages in the four-dimensional phase space $\{\vartheta_0, \varphi_0, \omega_x^0, \omega_y^0\}$ are [21]

$$\langle (\cdot) \rangle = \int_0^{\pi} \int_0^{2\pi} \int_{-\infty}^{\infty} \int_{-\infty}^{\infty} (\cdot) W_{st}(\vartheta_0, \varphi_0, \omega_x^0, \omega_y^0) \times \sin \vartheta_0 d\omega_x^0 d\omega_y^0 d\varphi_0 d\vartheta_0, \quad (3)$$

where

$$W_{st}(\vartheta_0, \varphi_0, \omega_x^0, \omega_y^0) = Z^{-1} e^{-(\eta\omega_x^0)^2 - (\eta\omega_y^0)^2 + \xi \cos \vartheta_0} \quad (4)$$

is the stationary distribution function in phase space [21],

$$Z = \int_0^{\pi} \int_0^{2\pi} \int_{-\infty}^{\infty} \int_{-\infty}^{\infty} e^{-(\eta\omega_x^0)^2 - (\eta\omega_y^0)^2 + \xi \cos \vartheta_0} \times \sin \vartheta_0 d\omega_x^0 d\omega_y^0 d\varphi_0 d\vartheta_0 = \frac{4\pi^2 \sinh \xi}{\xi \eta^2} \quad (5)$$

is the partition function, $\xi = 2\gamma H \eta^2 / \tau$, $\eta = [v\mu_0 M_S \tau / (2\gamma kT)]^{1/2}$, v is the volume of the particle, $\mu_0 = 4\pi \times 10^{-7} \text{ J A}^{-2} \text{ m}^{-1}$ in SI units, and kT is the thermal energy.

By using the uniformly convergent expansion of the elliptic function $\text{sn}^2(s|m)$ in Fourier series [38] we may represent the longitudinal component of vector \mathbf{u} given by Eq. (A5) as the Fourier series,

$$u_{\parallel}(t') = e_3 + \frac{E(m)(e_1 - e_3)}{K(m)} + \frac{2\pi^2(e_1 - e_3)}{K^2(m)} \times \sum_{n=1}^{\infty} \frac{nq^n(m)}{1 - q^{2n}(m)} \cos \frac{\pi ns}{K(m)}, \quad (6)$$

where

$$q^n(m) = \exp[-\pi K(1-m)/K(m)], \quad (7)$$

and $K(m)$ and $E(m)$ are the complete elliptic integrals of the first and second kind, respectively, and all other values are defined in Appendix A. Taking into account that $u_{\parallel}(t')$ from Eq. (6) depends on variables $\{\delta, P, l\}$ (see Appendix A), it is preferable to use these variables instead of $\{\vartheta_0, \omega_x^0, \omega_y^0\}$ in Eq. (3). The Jacobian of this transformation is (see Appendix B)

$$\left| \frac{\sin \vartheta_0 (\partial \vartheta_0, \partial \omega_x^0, \partial \omega_y^0)}{(\partial \delta, \partial P, \partial l)} \right| = \frac{1}{\eta^2 \sqrt{\xi} (e_1 - e_3)}. \quad (8)$$

Moreover, integration over φ in Eq. (3) gives the factor 2π as $u_{\parallel}(t')$ is independent of this angle. Thus, the $C_{\parallel}^{un}(t)$ can be written as ($t = t'\eta$)

$$C_{\parallel}^{un}(t) = C_{\parallel}^{un}(0) + \int_{-\xi+r^2}^{\infty} dP e^{-P+r^2} \int_{l_1}^{l_2} dl \sum_{n=1}^{\infty} c_n (\cos w_n t - 1), \quad (9)$$

where

$$w_n = \frac{\pi n \sqrt{\xi} (e_1 - e_3)}{2\eta K(m)}, \quad (10)$$

$$c_n = \frac{\pi^3 n^2 \sqrt{\xi} (e_1 - e_3)^3}{2K^3(m) \sinh \xi \sinh^2[\pi n K(1-m)/K(m)]}, \quad (11)$$

and [28,33]

$$C_{\parallel}^{un}(0) = 1 - \coth^2 \xi + \xi^{-2}. \quad (12)$$

The Fourier-Laplace transform of $C_{\parallel}^{un}(t)$ is

$$\begin{aligned} \tilde{C}_{\parallel}^{un}(z) &= \int_0^{\infty} e^{izt} C_{\parallel}^{un}(t) dt \\ &= \frac{i}{z} C_{\parallel}^{un}(0) - \frac{i}{z} \int_{-\xi+r^2}^{\infty} dP e^{-P+r^2} \\ &\quad \times \int_{l_1}^{l_2} dl \sum_{n=1}^{\infty} \frac{c_n w_n^2}{w_n^2 - z^2}. \end{aligned} \quad (13)$$

III. EQUILIBRIUM TRANSVERSE CORRELATION FUNCTION

For the transverse component $u_{\perp}(t')$ of vector \mathbf{u} given by Eq. (A13) we take into account that [38,39]

$$1 - a \operatorname{sn}^2(s|m) = \Theta^2(0) \frac{\Theta(s-\beta)\Theta(s+\beta)}{\Theta^2(s)\Theta^2(\beta)} \quad (14)$$

and

$$\Pi[a, \operatorname{am}(s|m), m] = \frac{\operatorname{sn}(\beta|m)}{\operatorname{cn}(\beta|m)\operatorname{dn}(\beta|m)} \left[u \frac{H'(\beta)}{H(\beta)} + \frac{1}{2} \ln \left(\frac{\Theta(s-\beta)}{\Theta(s+\beta)} \right) \right], \quad (15)$$

where

$$\beta = \operatorname{sn}^{-1}(\sqrt{a/m}|m) = F(\arcsin \sqrt{a/m}, m). \quad (16)$$

Thus, Eq. (A13) can now be expressed in terms of the Jacobian theta functions $H(\beta)$ and $\Theta(\beta)$ as

$$\begin{aligned} u_{\perp}(t') &= (1 - e_1^2)^{1/2} \frac{\Theta^2(0)}{2\Theta^2(s)} \left\{ e^{i[\varphi_0 + (s-\delta)\lambda]} \prod_{j=1,2} \frac{\Theta(s + \beta_j \varepsilon_j)}{\Theta(\beta_j)} \left[\frac{\Theta(\delta - \beta_j \varepsilon_j)}{\Theta(\delta + \beta_j \varepsilon_j)} \right]^{1/2} \right. \\ &\quad \left. + e^{-i[\varphi_0 + (s-\delta)\lambda]} \prod_{j=1,2} \frac{\Theta(s - \beta_j \varepsilon_j)}{\Theta(\beta_j)} \left[\frac{\Theta(\delta + \beta_j \varepsilon_j)}{\Theta(\delta - \beta_j \varepsilon_j)} \right]^{1/2} \right\}, \end{aligned} \quad (17)$$

where $\varphi_0 = \varphi(0)$ and

$$\lambda = i \left[\operatorname{sgn}(k+l) \frac{H'(\beta_1)}{H(\beta_1)} + \operatorname{sgn}(k-l) \frac{H'(\beta_2)}{H(\beta_2)} \right] \quad (18)$$

Here we use the fact that

$$\varepsilon_{1,2} = -\frac{ib_{1,2} \operatorname{sn}(\beta_{1,2}|m)}{\operatorname{cn}(\beta_{1,2}|m)\operatorname{dn}(\beta_{1,2}|m)} = \operatorname{sgn}(k \pm l). \quad (19)$$

Taking into account that

$$\begin{aligned} \int_0^{2\pi} u_{\perp}(0) u_{\perp}(t') d\varphi_0 &= 2\pi (1 - e_1^2) \frac{\Theta^4(0)}{4\Theta^2(\beta_1)\Theta^2(\beta_2)} \left\{ e^{i[(s-\delta)\lambda]} \frac{\Theta(s + \beta_1 \varepsilon_1)\Theta(s + \beta_2 \varepsilon_2)}{\Theta^2(s)} \frac{\Theta(\delta - \beta_1 \varepsilon_1)\Theta(\delta - \beta_2 \varepsilon_2)}{\Theta^2(\delta)} \right. \\ &\quad \left. + e^{-i[(s-\delta)\lambda]} \frac{\Theta(s - \beta_1 \varepsilon_1)\Theta(s - \beta_2 \varepsilon_2)}{\Theta^2(s)} \frac{\Theta(\delta + \beta_2 \varepsilon_2)\Theta(\delta + \beta_1 \varepsilon_1)}{\Theta^2(\delta)} \right\} \end{aligned} \quad (20)$$

and on using the uniformly convergent Fourier series [40]

$$\frac{\Theta(u \pm \beta_1)\Theta(u \pm \beta_2)}{\Theta^2(u)} = -\frac{\pi^3 H(\beta_1)H(\beta_2)}{4K^3(m)\sqrt{m(1-m)}} \sum_{n=-\infty}^{\infty} \frac{\left\{n \pm \frac{iK(m)}{\pi} \left[\frac{H'(\beta_1)}{H(\beta_1)} + \frac{H'(\beta_2)}{H(\beta_2)} \right] \right\} \exp\left[\frac{i\pi nu}{K(m)}\right]}{\sinh\left(\frac{\pi}{2K(m)}[2nK(1-m) \mp i\beta_1 \mp i\beta_2]\right)}, \quad (21)$$

we can calculate the equilibrium average in the manner outlined above. Thus, we obtain the expression for the transverse equilibrium correlation function and its spectrum,

$$C_{\perp}^{un}(t) = C_{\perp}^{un}(0) + \int_{-\xi+r^2}^{\infty} dP e^{-P+r^2} \int_{l_1}^{l_2} dl \sum_{n=1}^{\infty} c'_n (\cos w'_n t - 1) \quad (22)$$

and

$$\tilde{C}_{\perp}^{un}(z) = \frac{i}{z} C_{\perp}^{un}(0) - \frac{i}{z} \int_{-\xi+r^2}^{\infty} dP e^{-P+r^2} \int_{l_1}^{l_2} dl \sum_{n=1}^{\infty} \frac{c'_n w_n'^2}{w_n'^2 - z^2}, \quad (23)$$

where

$$w'_n = \frac{[\lambda + \pi n/K(m)]}{2\eta} \sqrt{\xi(e_1 - e_3)}, \quad (24)$$

$$c'_n = -\frac{\pi^3 \sqrt{\xi(e_1 - e_3)^3} [n + \lambda K(m)/\pi]^2}{8K^3(m) \sinh \xi \sinh^2\left[\frac{\pi}{2K(m)}[2nK(1-m) - i\beta_1 \varepsilon_1 - i\beta_2 \varepsilon_2]\right]}, \quad (25)$$

and [28,33]

$$C_{\perp}^{un}(0) = \xi^{-1} \coth \xi - \xi^{-2}. \quad (26)$$

IV. ROTATIONAL DIFFUSION IN A DC MAGNETIC FIELD AND MAGNETIC SUSCEPTIBILITY

The presented correlation functions can be employed to describe the relaxation dynamics in the processes of magnetization or magnetization reversal. These dynamics correspond to the process of reaching thermodynamic equilibrium in a spin system. For example, the small variation of the external field from $\mathbf{H} + \Delta\mathbf{H}$ to \mathbf{H} results in a disturbance of the equilibrium state of the spin system, which changes and the system relaxes to a new equilibrium state. Magnetic relaxation determines the width of the lines of FMR and NR. Bloch [34] introduced the phenomenological approach that the evolution of the magnetization towards equilibrium was exponential, however embodying two distinct time constants: T_{\parallel} for the longitudinal component and T_{\perp} for the transverse component. The time evolution of a correlation function of microscopic variables should be consistent with the concept that these variables, separated by large time scales, should be uncorrelated. This concept is reflected in the Lorentz diffusion model, in which the longitudinal and transverse correlation functions are expressed as [41]

$$C_g(t) = C_g^{un}(t) e^{-t/T_g} + \frac{1}{T_g} \int_0^t C_g^{un}(t') e^{-t'/T_g} dt', \quad (27)$$

or

$$\dot{C}_g(t) = \dot{C}_g^{un}(t) e^{-t/T_g}, \quad g = \parallel, \perp, \quad (28)$$

where the correlation functions $C_{\parallel}^{un}(t)$ and $C_{\perp}^{un}(t)$ correspond to the undamped dynamics of the magnetization and are given by Eqs. (9) and (22). The model is commonly used to describe orientational relaxation in gases and liquids by taking into account inertial effects [41].

According to linear response theory [42,43], there is a relationship between the responses to a small change $\Delta\mathbf{H}$ in the external field \mathbf{H} , described by equilibrium correlation functions, and the responses to a small probing alternating field $\mathbf{H}_{ac} e^{i\omega t}$ applied additionally to the external field \mathbf{H} , since the components $\chi_g(\omega)$ of the magnetic susceptibility tensor can be expressed in terms of the appropriate equilibrium correlation functions:

$$\chi_g(\omega) = C_g(0) + i\omega \tilde{C}_g(\omega), \quad (29)$$

where $C_g(0) = C_g^{un}(0)$. The linear response theory assumes that the perturbation energy of a nanomagnet in an external field is smaller than the thermal energy kT , or $v\mu_0 M_S \Delta H/kT < 1$ ($v\mu_0 M_S H_{ac}/kT < 1$). Here the values $\Delta H = |\Delta\mathbf{H}|$ and $H_{ac} = |\mathbf{H}_{ac}|$ (not the absolute value of the applied uniform external field $H = |\mathbf{H}|$) are important. Thus, the condition of the linear response is easily satisfied for nanoparticles having small volumes v at small values of ΔH and H_{ac} . Equations (27) and (29) allow us to evaluate the components of the complex magnetic susceptibility tensor, viz., $\chi_{\parallel}(\omega) = \chi_{ZZ}(\omega)$ and $\chi_{\perp}(\omega) = \chi_{XX}(\omega) = \chi_{YY}(\omega)$ for the spin system in the dc field \mathbf{H} ,

$$\chi_g(\omega) = C_g^{un}(0) + iz \tilde{C}_g^{un}(z), \quad (30)$$

where $z = \omega + i/T_g$.

V. RESULTS AND DISCUSSION

The real $\bar{\chi}'_g(\omega) = C_g^{un}(0) \chi'_g(\omega)/\chi_g$ and imaginary $\bar{\chi}''_g(\omega) = C_g^{un}(0) \chi''_g(\omega)/\chi_g$ parts of the susceptibility tensor components are shown in Figs. 1–6 for various

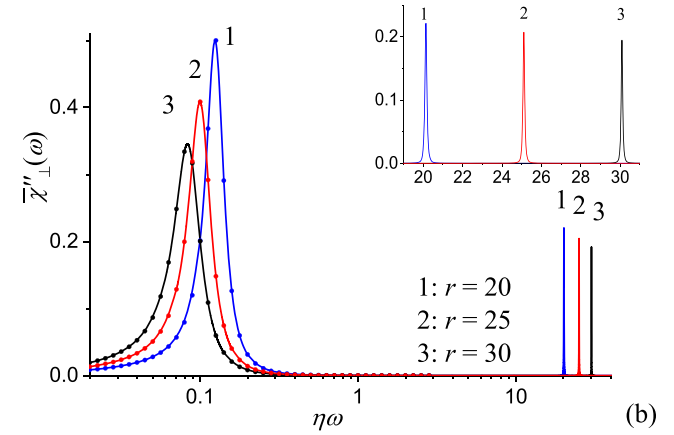
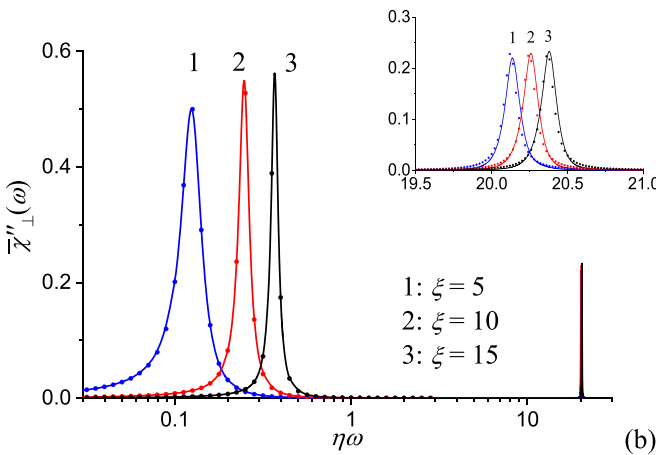
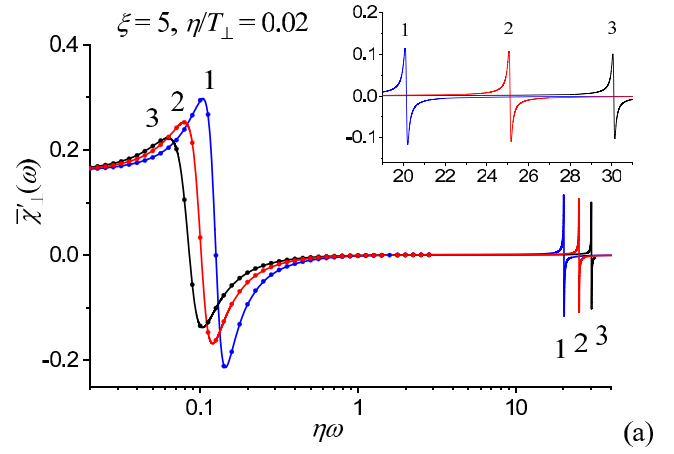
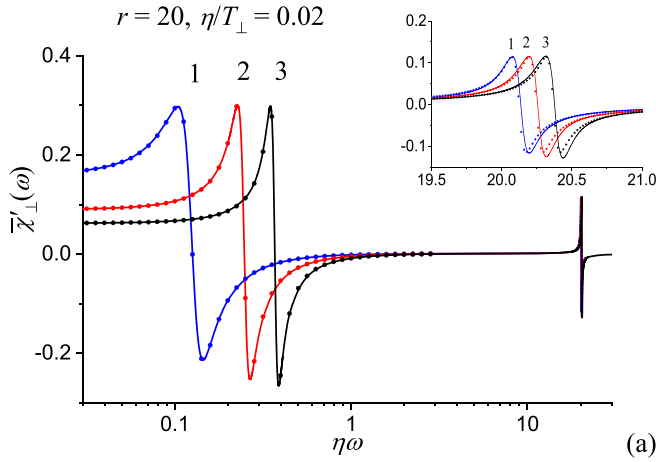


FIG. 1. Real $\bar{\chi}'_{\perp}(\omega) = C_{\perp}^{un}(0)\chi'_{\perp}(\omega)/\chi_{\perp}$ (a) and imaginary $\bar{\chi}''_{\perp}(\omega) = C_{\perp}^{un}(0)\chi''_{\perp}(\omega)/\chi_{\perp}$ (b) parts of the transverse component of the susceptibility tensor vs $\eta\omega$ for $r = 20$, $\eta/T_{\perp} = 0.02$, and various values of field parameter ξ . Solid lines: Eqs. (23) and (30); symbols: approximate Eq. (31) with $\eta/T_{\perp} = 0.02$ for FMR and $\eta/T_{\perp} = \eta/T_{\perp}^{\text{eff}} = 0.05$ for NR (inset).

values of the parameters r , ξ , and T_g . Here $\chi_g = \chi'_g(0)$ and $C_g^{un}(0)$ are given by Eqs. (12) and (26). The parameter $\xi = v\mu_0 M_S H / (kT)$ is the energy of a particle of volume v with a magnetic moment vM_S in a uniform external field H , expressed in units of thermal energy kT . For example, for cobalt ($M_S = 1.4 \times 10^6$ A/m) nanoparticle ($v = 10^{-24}$ m³) in an external field $H \sim 450$ A/m (~ 5.6 Oe) we have $\xi \approx 1.9$ at $T = 30$ K. The low frequency band is observed in the transverse component $\bar{\chi}''_{\perp}(\omega)$ and corresponds to ferromagnetic resonance. An approximate equation for the transverse component $\chi_{\perp}(\omega)$ can be obtained by applying the method of successive approximations based on the linearization of the ILLG equation [37]. The resultant equation for $\chi_{\perp}(\omega)$ with negligible α is [44]

$$\chi_{\perp}(\omega) = \frac{\omega_M[\omega_H - \tau(\omega + i/T_{\perp})^2]}{[\omega_H - \tau(\omega + i/T_{\perp})^2]^2 - (\omega + i/T_{\perp})^2}, \quad (31)$$

where $\omega_H = \gamma H$ and $\omega_M = \gamma M_S$. Here the time constant T_{\perp} is introduced by the substitution $\omega \rightarrow \omega + i/T_{\perp}$ to take into account the statistical properties of the spin system, namely,

FIG. 2. Real $\bar{\chi}'_{\perp}(\omega) = C_{\perp}^{un}(0)\chi'_{\perp}(\omega)/\chi_{\perp}$ (a) and imaginary $\bar{\chi}''_{\perp}(\omega) = C_{\perp}^{un}(0)\chi''_{\perp}(\omega)/\chi_{\perp}$ (b) parts of the transverse component of the susceptibility tensor vs $\eta\omega$ for $\xi = 5$, $\eta/T_{\perp} = 0.02$, and various values of inverse inertia parameter r . Solid lines: Eqs. (23) and (30); symbols: approximate Eq. (31).

the evolution of the system towards equilibrium, characterized by the transverse relaxation time T_{\perp} . In Figs. 1–3 the curves $\bar{\chi}'_{\perp}(\omega)$ and $\bar{\chi}''_{\perp}(\omega)$ are approximated to good accuracy by using Eq. (31). However, while the same time constant $\eta T_{\perp} = 0.02$ was used for the exact calculation [Eqs. (22) and (28)] and approximation [Eq. (29)] in the FMR region, different time constants, namely, $\eta T_{\perp} = 0.02$ for the exact calculation and $\eta T_{\perp} = \eta T_{\perp}^{\text{eff}} = 0.05$ for the approximation were used in the NR region to obtain a correspondence between the exact calculation and the approximation (see Fig. 1). The resonant frequency of the spectrum $\bar{\chi}''_{\perp}(\omega)$ can be estimated as $\eta\omega_{\text{FMR}} \sim \eta\omega_H = \xi/(2r)$. A second resonance band appears in the spectrum $\bar{\chi}''_{\perp}(\omega)$ at ultrahigh frequencies due to the nutation of the magnetization (nutation resonance). While FMR (low frequency band in Figs. 1–3) is well studied, NR (high frequency band in Figs. 1–3) is a rather new subject of experimental research. In a rough approximation, the NR frequency ω_{NR} is determined by the inertial parameter τ , namely $\omega_{\text{NR}} \sim \tau^{-1}$ ($\eta\omega_{\text{NR}} \sim r$). Recent experimental studies [1] have shown that this frequency lies in the THz frequency range $\omega_{\text{NR}} \sim 10^{11} - 10^{13}$ Hz. NR was recently detected at THz frequencies in NiFe, CoFeB, and Co ferromagnetic films [1,25]. Detailed theoretical investigations of NR frequencies and their

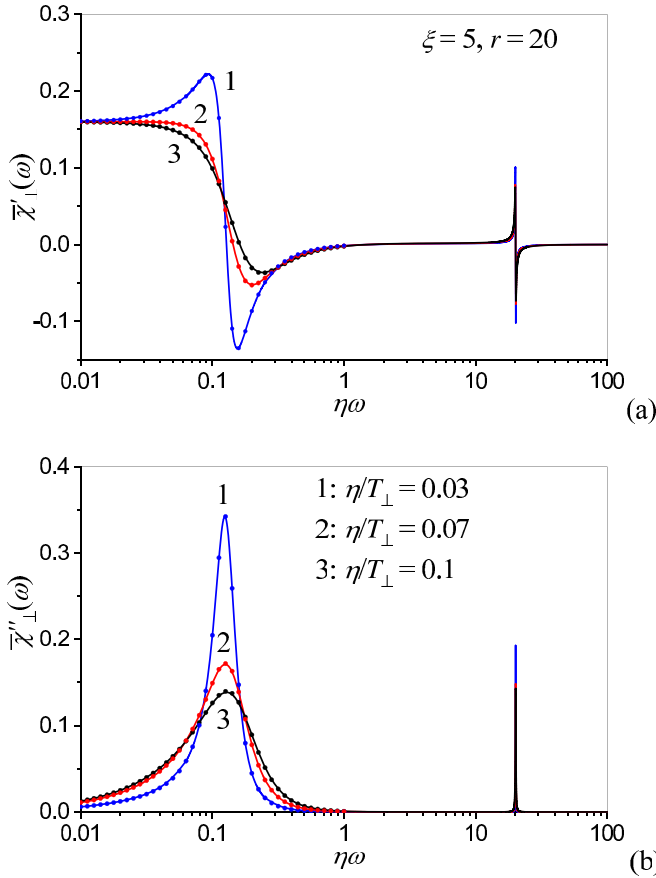


FIG. 3. Real $\bar{\chi}'_{\perp}(\omega) = C_{\perp}^{m}(0)\chi'_{\perp}(\omega)/\chi_{\perp}$ (a) and imaginary $\bar{\chi}''_{\perp}(\omega) = C_{\perp}^{m}(0)\chi''_{\perp}(\omega)/\chi_{\perp}$ (b) parts of the transverse component of the susceptibility tensor vs $\eta\omega$ for $r = 20$, $\xi = 5$, and various values of longitudinal relaxation time η/T_{\perp} . Solid lines: Eqs. (23) and (30); symbols: approximate Eq. (31).

dependence on the parameters of nanoparticles and external field are given in [23,24]. The increase of r (decrease of inertia) shifts the resonance curve toward higher frequencies (see Fig. 2). As shown in Fig. 2 the increase of r leads to a decrease in the amplitude of the resonance, which disappears as $r \rightarrow \infty$. The parameter η/T_{\perp} affects the width of the bands (see Fig. 3). At $\eta/T_{\perp} > 0.2$ one could also see a change in the resonant frequency. However, we do not consider this case here, since the resonant frequency is well determined by the deterministic undamped ILLG equation [23,24], which is the case for $\eta/T_{\perp} \rightarrow 0$.

The spectra of the real $\bar{\chi}'_{\parallel}(\omega)$ and imaginary $\bar{\chi}''_{\parallel}(\omega)$ parts of the longitudinal susceptibility are plotted in Figs. 4–6 for the NR region. According to Eqs. (13) and (30) the complex susceptibility $\chi_{\parallel}(\omega)$ can be presented as a sum of Lorentzian resonance curves. Hence, the resultant curve can be accurately described by a single Lorentzian resonance curve, but with effective resonant frequency ω_{eff} and half width $1/T_{\parallel}^{\text{eff}}$, namely

$$\chi_{\parallel}(\omega) = \frac{\omega_M \omega_{\text{eff}}}{\omega_{\text{eff}}^2 - (\omega + i/T_{\parallel}^{\text{eff}})^2}. \quad (32)$$

The values of effective resonant frequencies $\eta\omega_{\text{eff}}$ and half widths $\eta/T_{\parallel}^{\text{eff}}$ are given in Table I for various curves plotted in

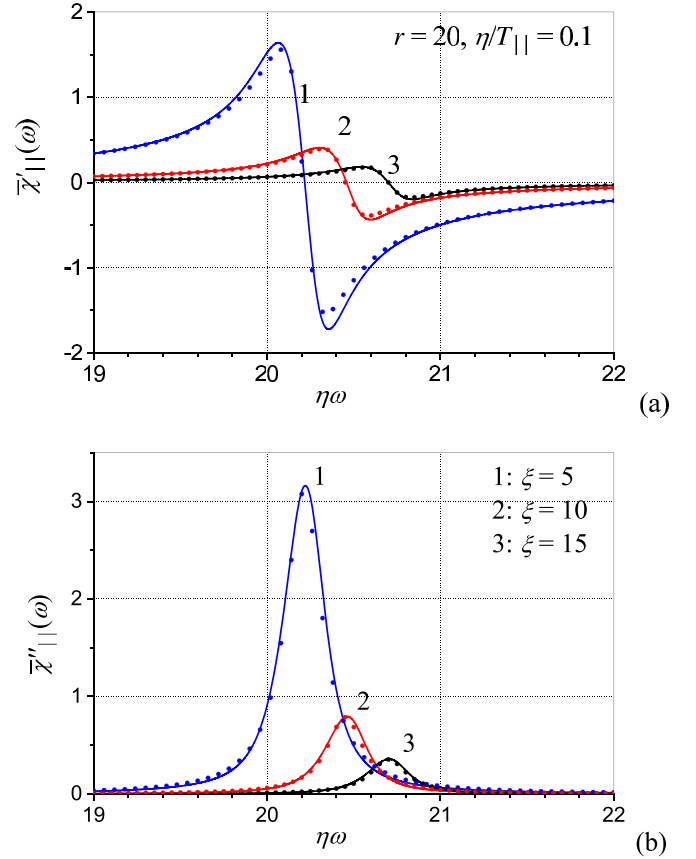


FIG. 4. Real $\bar{\chi}'_{\parallel}(\omega) = C_{\parallel}^{m}(0)\chi'_{\parallel}(\omega)/\chi_{\parallel}$ (a) and imaginary $\bar{\chi}''_{\parallel}(\omega) = C_{\parallel}^{m}(0)\chi''_{\parallel}(\omega)/\chi_{\parallel}$ (b) parts of the longitudinal component of the susceptibility tensor vs $\eta\omega$ for $r = 20$, $\eta/T_{\parallel} = 0.1$, and various values of field parameter ξ [Eqs. (13) and (30)].

Figs. 4–6. Formally, Eq. (32) follows from Eq. (31) by substitution $\omega_H \rightarrow 0$, $\tau^{-1} \rightarrow \omega_{\text{eff}}$ and $T_{\perp} \rightarrow T_{\parallel} \rightarrow T_{\parallel}^{\text{eff}}$. Moreover, the values ω_{eff} and $T_{\parallel}^{\text{eff}}$ can be roughly estimated as $\omega_{\text{eff}} \sim \tau^{-1}$ and $T_{\parallel}^{\text{eff}} \sim T_{\parallel}$.

VI. CONCLUSION

We have shown how the correlation functions and magnetic susceptibilities of the spin system in a strong magnetic field can be exactly calculated by expanding the deterministic magnetization trajectories into a Fourier series and averaging the result over all possible initial conditions applying the stationary Boltzmann distribution function. The main result is that the susceptibility is expressed as the sum of a discrete set of Lorentz-type curves. Furthermore, we have demonstrated that the simple analytical Eq. (31), obtained by using the method

TABLE I. Effective parameters used in Figs. 4–6.

Figure	4			5			6		
Curve	1	2	3	1	2	3	1	2	3
ω_{eff}	20.21	20.45	20.70	20.21	25.17	30.14	20.31	20.21	20.2
$\eta/T_{\parallel}^{\text{eff}}$	0.13	0.13	0.13	0.13	0.12	0.115	0.055	0.13	0.5

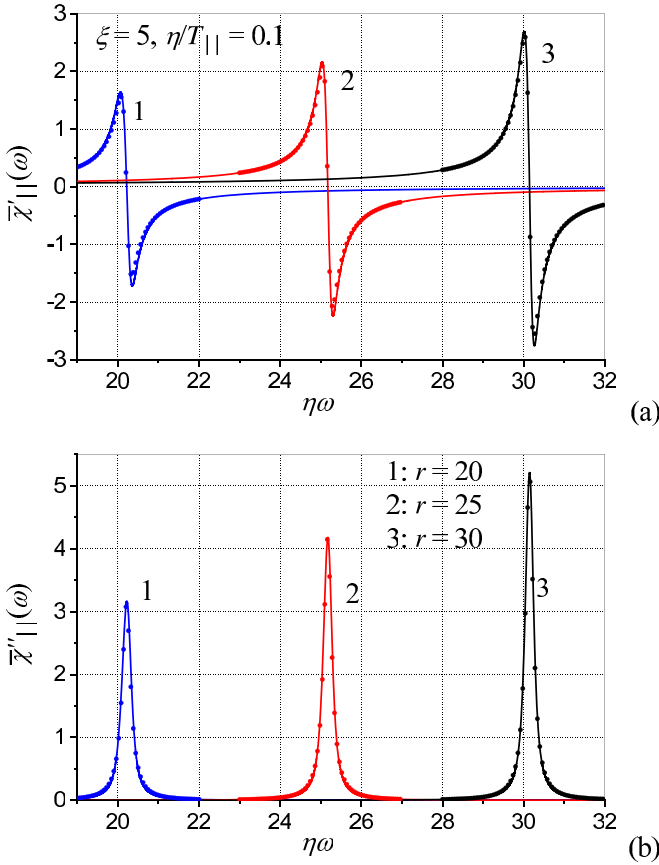


FIG. 5. Real $\bar{\chi}'_{||}(\omega) = C_{||}^{un}(0)\chi'_{||}(\omega)/\chi_{||}$ (a) and imaginary $\bar{\chi}''_{||}(\omega) = C_{||}^{un}(0)\chi''_{||}(\omega)/\chi_{||}$ (b) parts of the longitudinal component of the susceptibility tensor vs $\eta\omega$ for $\xi = 5$, $\eta/T_{||} = 0.1$ and various values of inverse inertia parameter r [Eqs. (13) and (30)].

of successive approximations based on the linearization of the ILLG equation [37], describes the main features of the transverse complex susceptibility in the FMR and NR regions. Moreover, the simplified Eq. (32) serves as a good approximation for the longitudinal susceptibility in the NR region. The exact solution is also useful for evaluating the accuracy of various approximations.

ACKNOWLEDGMENTS

We thank Y. P. Kalmykov for useful comments and suggestions. The work was supported by the Foundation for the Advancement of Theoretical Physics and Mathematics “BASIS” (Grant No. 22-1-1-28-1).

APPENDIX A: SOLUTION OF UNDAMPED ILLG EQUATION

The vector Eq. (2) can be transformed to the system of two scalar differential equations for the polar angle $\vartheta(t)$ [or for $u_{||}(t) = \cos \vartheta(t)$] and for the azimuthal angle $\varphi(t)$ [22,35,45,46],

$$\frac{du_{||}}{dt'} = \pm \sqrt{\Phi(u_{||})}, \quad (\text{A1})$$

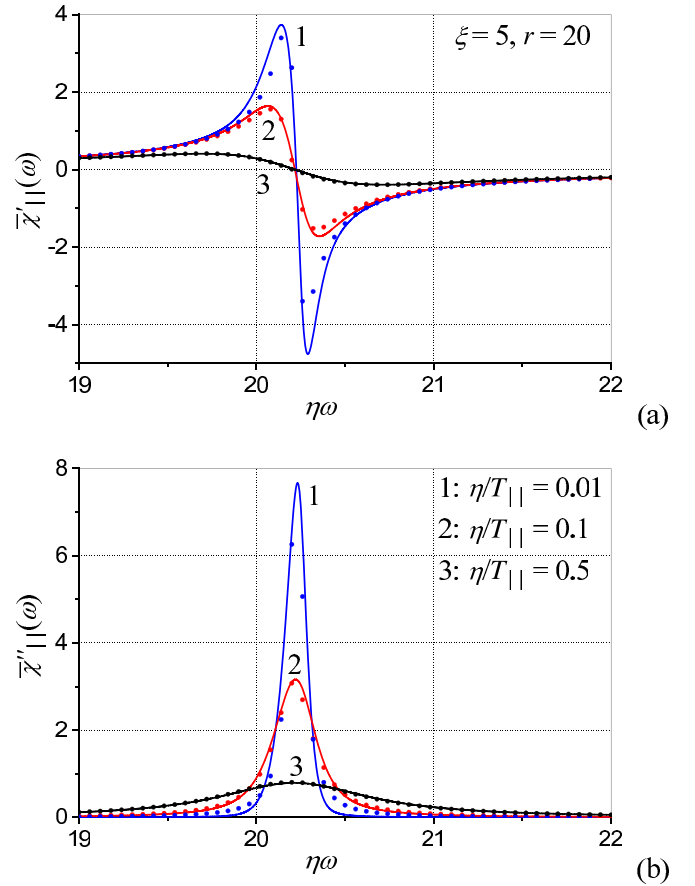


FIG. 6. Real $\bar{\chi}'_{||}(\omega) = C_{||}^{un}(0)\chi'_{||}(\omega)/\chi_{||}$ (a) and imaginary $\bar{\chi}''_{||}(\omega) = C_{||}^{un}(0)\chi''_{||}(\omega)/\chi_{||}$ (b) parts of the longitudinal component of the susceptibility tensor vs $\eta\omega$ for $r = 20$, $\xi = 5$ and various values of longitudinal relaxation time $\eta/T_{||}$ [Eqs. (13) and (30)].

$$\frac{d\varphi}{dt'} = -\frac{1}{2} \left(\frac{l+r}{1+u_{||}(t')} + \frac{l-r}{1-u_{||}(t')} \right), \quad (\text{A2})$$

where

$$\Phi(u_{||}) = (\xi u_{||} + P)(1 - u_{||}^2) + 2lru_{||} - l^2 - r^2 \quad (\text{A3})$$

is the third-order polynomial, $r = \eta/\tau$ and $t' = t/\eta$. Equation (A3) also contains two first integrals,

$$l = \eta\Omega_Z = \text{const}, \quad P = \eta^2\Omega^2 - \xi u_{||} = \text{const}, \quad (\text{A4})$$

where $\Omega^2 = (\dot{\mathbf{u}} \cdot \dot{\mathbf{u}}) + \tau^{-2}$ and $\boldsymbol{\Omega} = (\Omega_X, \Omega_Y, \Omega_Z) = [\dot{\mathbf{u}} \times \mathbf{u}] + \tau^{-1}\mathbf{u}$. The sign of $\dot{u}_{||}(t')$ is determined by the initial condition $\dot{u}_{||}(0) = -\dot{\vartheta}(0)\sin \vartheta(0)$. It is known from the theory of elliptic functions [38] that the solution of Eq. (A1) with the initial condition $u_{||}(0) = \cos \theta(0)$ can be expressed in terms of the Jacobian doubly periodic function $\text{sn}(u|m)$ [39], viz.

$$u_{||}(t') = e_1 - (e_1 - e_2)\text{sn}^2(s|m), \quad (\text{A5})$$

where

$$s = \frac{t'}{2} \sqrt{\xi(e_1 - e_3)} + \delta, \quad m = \frac{e_1 - e_2}{e_1 - e_3}, \quad (\text{A6})$$

and e_1 , e_2 , and e_3 are the real roots of the polynomial $\Phi(u_{\parallel})$,

$$e_1 = 2p \cos(\Xi/3) - P/3\xi, \quad (\text{A7})$$

$$e_{2,3} = -2p \cos[(\Xi \pm \pi)/3] - P/3\xi, \quad (\text{A8})$$

where

$$p = \sqrt{\left(\frac{P}{3\xi}\right)^2 + \frac{2lr}{3\xi} + \frac{1}{3}},$$

$$\Xi = \arccos \left[\frac{1}{p^3} \left(\frac{P}{3\xi} \left(1 - \frac{lr}{\xi} \right) - \left(\frac{P}{3\xi} \right)^3 - \frac{l^2 + r^2}{2\xi} \right) \right].$$

The constant of integration δ is found from the equation

$$\cos \vartheta(0) = e_1 - (e_1 - e_2) \text{sn}^2(\delta|m) \quad (\text{A9})$$

and is given by

$$\delta = \text{sn}^{-1}(\sqrt{[e_1 - \cos \vartheta(0)]/(e_1 - e_2)}|m), \quad (\text{A10})$$

where $x = \text{sn}^{-1}(y|m)$ is the inverse of the Jacobian function $y = \text{sn}(x|m)$.

The parameter P lies in the interval $[r^2 - \xi, \infty]$, whereas l lies in the interval $[l_1, l_2]$, which can be determined from the following equation:

$$\begin{aligned} \Phi(u_m) = & -r^2 - \frac{2}{3\xi}Plr - l^2 + \frac{2P}{3} \left(1 - \frac{P^2}{9\xi^2} \right) \\ & + \frac{2}{27\xi^2} (P^2 + 6\xi lr + 3\xi^2)^{3/2} = 0, \end{aligned} \quad (\text{A11})$$

where

$$u_m = \frac{1}{3\xi} (\sqrt{P^2 + 6\xi lr + 3\xi^2} - P) \quad (\text{A12})$$

is the value of u at which the function $\phi(u)$ from Eq. (A3) reaches a maximum in the interval $[-1, 1]$. The standard solution of Eq. (A11) yields four roots, l_i , $i = 1, 2, 3, 4$ [35,47]. We must choose from the roots those satisfying Eq. (A11) and yielding the values of l_1 and l_2 .

Integration of Eq. (A2) and substitution of the result into the equation $u_{\perp}(t') = \sqrt{1 - u_{\parallel}^2(t')} \cos \varphi(t')$ then yields

$$\begin{aligned} u_{\perp}(t') = & \left\{ (1 - e_1^2) \prod_{j=1,2} [1 - a_j \text{sn}^2(s|m)] \right\}^{1/2} \\ & \times \cos \left\{ \varphi(0) + \sum_{j=1,2} b_j \{ \Pi[a_j, \text{am}(s, m)|m] \right. \\ & \left. - \Pi[a_j, \text{am}(\delta, m)|m] \right\}, \end{aligned} \quad (\text{A13})$$

where $a_{1,2} = \frac{e_1 - e_2}{e_1 \pm 1}$, $b_{1,2} = -\frac{l \pm r}{(1 \pm e_1) \sqrt{\xi(e_1 - e_3)}}$, and s is defined by Eq. (A6). Here $\Pi(a, \phi, m)$ is the incomplete elliptic integral of the third kind [39], a_1 and b_1 correspond to the sign “+,” and $0 < a_1 < 1$, $-\infty < a_2 < 0$.

APPENDIX B: JACOBIAN OF THE TRANSFORMATION

We first use the following transformation: $\{\vartheta_0, \omega_x^0, \omega_y^0\} \rightarrow \{u, P, l\}$, which is given by the following equations:

$$u_0 = \cos \vartheta_0, \quad (\text{B1})$$

$$l = r \cos \vartheta_0 - \eta \omega_y^0 \sin \vartheta_0, \quad (\text{B2})$$

$$P = (\eta \omega_x^0)^2 + (\eta \omega_y^0)^2 + r^2 - \xi \cos \vartheta_0. \quad (\text{B3})$$

The Jacobian of this transformation is

$$\begin{aligned} J = & \left| \begin{array}{ccc} (\partial \vartheta_0, \partial \omega_y^0, \partial \omega_x^0) \\ (\partial u_0, \partial l, \partial P) \end{array} \right| = \left| \begin{array}{ccc} \partial_{u_0} \vartheta_0 & 0 & 0 \\ \partial_{u_0} \omega_y^0 & \partial_l \omega_y^0 & 0 \\ \partial_{u_0} \omega_x^0 & \partial_l \omega_x^0 & \partial_P \omega_x^0 \end{array} \right| \\ = & |\partial_{u_0} \vartheta_0 \partial_l \omega_y^0 \partial_P \omega_x^0|. \end{aligned} \quad (\text{B4})$$

We have from Eqs. (B1)–(B3)

$$\partial_{u_0} \vartheta_0 = -\frac{1}{\sqrt{1 - u_0^2}}, \quad (\text{B5})$$

$$\partial_l \omega_y^0 = -\frac{1}{\eta \sqrt{1 - u_0^2}}, \quad (\text{B6})$$

$$\partial_P \omega_x^0 = \frac{\sqrt{1 - u_0^2}}{2\eta \sqrt{\Phi(u_0)}}. \quad (\text{B7})$$

By substituting Eqs. (B5)–(B7) into Eq. (B4) we obtain

$$J \sqrt{1 - u_0^2} = \frac{1}{2\eta^2 \sqrt{\Phi(u_0)}}. \quad (\text{B8})$$

Next, by considering integration over u_0 as an internal integral (at given P and l), we apply the substitution $u_0 = e_1 - (e_1 - e_2) \text{sn}^2(\delta|m)$ [see Eq. (A5)]. Taking into account that

$$du_0 = \frac{\partial u_0}{\partial \delta} d\delta = \frac{2}{\sqrt{\xi(e_1 - e_3)}} \frac{\partial u_{\parallel}}{\partial t'} \Big|_{t'=0} d\delta = \frac{2\sqrt{\Phi(u_0)}}{\sqrt{\xi(e_1 - e_3)}} d\delta, \quad (\text{B9})$$

we obtain Eq. (8).

[1] K. Neeraj, N. Awari, S. Kovalev, D. Polley, N. Z. Hagström, S. S. P. K. Arekapudi, A. Semisalova, K. Lenz, B. Green, J.-C. Deinert, I. Ilyakov, M. Chen, M. Bowatna, V. Scalera, M. D’Aquino, C. Serpico, O. Hellwig, J.-E. Wegrowe, M. Gensch, and S. Bonetti, Inertial spin dynamics in ferromagnets, *Nat. Phys.* **17**, 245 (2020).

[2] K. Jhuria, J. Hohlfeld, A. Pattabi, E. Martin, A. Y. A. Cyrdova, X. Shi, R. L. Conte, S. Petit-Watelot, J. C. Rojas-Sanchez, G. Malinowski, S. Mangin, A. Lemaotre, M. Hehn, J. Bokor, R. B. Wilson, and J. Gorchon, Spin-orbit torque switching of a ferromagnet with picosecond electrical pulses, *Nat. Electron.* **3**, 680 (2020).

- [3] D. Khusyainov, S. Ovcharenko, M. Gaponov, A. Buryakov, A. Klimov, N. Tiercelin, P. Pernod, V. Nozdryn, E. Mishina, A. Sigov, and V. Preobrazhensky, Polarization control of THz emission using spin-reorientation transition in spintronic heterostructure, *Sci. Rep.* **11**, 697 (2021).
- [4] A. Kirilyuk, A. V. Kimel, and T. Rasing, Ultrafast optical manipulation of magnetic order, *Rev. Mod. Phys.* **82**, 2731 (2010).
- [5] M.-C. Ciornei, J. M. Rubí, and J.-E. Wegrowe, Magnetization dynamics in the inertial regime: Nutation predicted at short time scales, *Phys. Rev. B* **83**, 020410(R) (2011).
- [6] M. Fähnle, D. Steiauf, and C. Illg, Generalized Gilbert equation including inertial damping: Derivation from an extended breathing Fermi surface model, *Phys. Rev. B* **84**, 172403 (2011).
- [7] J.-E. Wegrowe and M.-C. Ciornei, Magnetization dynamics, gyromagnetic relation, and inertial effects, *Am. J. Phys.* **80**, 607 (2012).
- [8] E. Olive, Y. Lansac, and J.-E. Wegrowe, Beyond ferromagnetic resonance: The inertial regime of the magnetization, *Appl. Phys. Lett.* **100**, 192407 (2012).
- [9] S. Bhattacharjee, L. Nordström, and J. Fransson, Atomistic Spin Dynamic Method with both Damping and Moment of Inertia Effects Included from First Principles, *Phys. Rev. Lett.* **108**, 057204 (2012).
- [10] D. Böttcher and J. Henk, Significance of nutation in magnetization dynamics of nanostructures, *Phys. Rev. B* **86**, 020404(R) (2012).
- [11] E. Olive, Y. Lansac, M. Meyer, M. Hayoun, and J.-E. Wegrowe, Deviation from the Landau-Lifshitz-Gilbert equation in the inertial regime of the magnetization, *J. Appl. Phys.* **117**, 213904 (2015).
- [12] T. Kikuchi and G. Tatara, Spin dynamics with inertia in metallic ferromagnets, *Phys. Rev. B* **92**, 184410 (2015).
- [13] J.-E. Wegrowe and E. Olive, The magnetic monopole and the separation between fast and slow magnetic degrees of freedom, *J. Phys.: Condens. Matter* **28**, 106001 (2016).
- [14] R. Mondal, M. Berritta, A. K. Nandy, and P. M. Oppeneer, Relativistic theory of magnetic inertia in ultrafast spin dynamics, *Phys. Rev. B* **96**, 024425 (2017).
- [15] R. Mondal, M. Berritta, and P. M. Oppeneer, Generalization of Gilbert damping and magnetic inertia parameter as a series of higher-order relativistic terms, *J. Phys.: Condens. Matter* **30**, 265801 (2018).
- [16] D. Thonig, O. Eriksson, and M. Pereiro, Magnetic moment of inertia within the torque-torque correlation model, *Sci. Rep.* **7**, 931 (2017).
- [17] S. Giordano and P.-M. Déjardin, Derivation of magnetic inertial effects from the classical mechanics of a circular current loop, *Phys. Rev. B* **102**, 214406 (2020).
- [18] Y. Li, V. V. Naletov, O. Klein, J. L. Prieto, M. Muñoz, V. Cros, P. Bortolotti, A. Anane, C. Serpico, and G. de Loubens, Nutation Spectroscopy of a Nanomagnet Driven into Deeply Nonlinear Ferromagnetic Resonance, *Phys. Rev. X* **9**, 041036 (2019).
- [19] R. Mondal, Theory of magnetic inertial dynamics in two-sublattice ferromagnets, *J. Phys.: Condens. Matter* **33**, 275804 (2021).
- [20] M. Cherkasskii, M. Farle, and A. Semisalova, Nutation resonance in ferromagnets, *Phys. Rev. B* **102**, 184432 (2020).
- [21] S. V. Titov, W. T. Coffey, Y. P. Kalmykov, M. Zarifakis, and A. S. Titov, Inertial magnetization dynamics of ferromagnetic nanoparticles including thermal agitation, *Phys. Rev. B* **103**, 144433 (2021).
- [22] S. V. Titov, W. T. Coffey, Y. P. Kalmykov, and M. Zarifakis, Deterministic inertial dynamics of the magnetization of nanoscale ferromagnets, *Phys. Rev. B* **103**, 214444 (2021).
- [23] S. V. Titov, W. J. Dowling, and Yu. P. Kalmykov, Ferromagnetic and nutation resonance frequencies of nanomagnets with various magnetocrystalline anisotropies, *J. Appl. Phys.* **131**, 193901 (2022).
- [24] M. Cherkasskii, I. Barsukov, R. Mondal, M. Farle, and A. Semisalova, Theory of inertial spin dynamics in anisotropic ferromagnets, *Phys. Rev. B* **106**, 054428 (2022).
- [25] V. Unikandanunni, R. Medapalli, M. Asa, E. Albisetti, D. Petti, R. Bertacco, E. E. Fullerton, and S. Bonetti, Inertial Spin Dynamics in Epitaxial Cobalt Films, *Phys. Rev. Lett.* **129**, 237201 (2022).
- [26] K. Neeraj, M. Pancaldi, V. Scalera, S. Perna, M. D'Aquino, C. Serpico, and S. Bonetti, Magnetization switching in the inertial regime, *Phys. Rev. B* **105**, 054415 (2022).
- [27] J. Anders, C. R. J. Sait, and S. A. R. Horsley, Quantum Brownian motion for magnets, *New J. Phys.* **24**, 033020 (2022).
- [28] S. V. Titov, W. J. Dowling, A. S. Titov, S. A. Nikitov, and M. Cherkasskii, Inertial dynamics and equilibrium correlation functions of magnetization at short times, *Phys. Rev. B* **107**, 104416 (2023).
- [29] L. Néel, Influence des fluctuations thermiques sur l'aimantation de grains ferromagnétiques très fins, *C. R. Acad. Sci. Paris* **228**, 664 (1949).
- [30] L. Néel, Théorie du traînage magnétique des ferromagnétiques en grains fins avec applications aux terres cuites, *Ann. Geophys.* **5**, 99 (1949).
- [31] W. F. Brown, Jr., Thermal fluctuations of a single-domain particle, *Phys. Rev.* **130**, 1677 (1963).
- [32] W. F. Brown, Jr., Thermal fluctuations of fine ferromagnetic particles, *IEEE Trans. Magn.* **15**, 1196 (1979).
- [33] W. T. Coffey, Yu. P. Kalmykov, and S. V. Titov, *Thermal Fluctuations and Relaxation Processes in Nanomagnets* (World Scientific, Singapore, 2020).
- [34] D. Forster, *Hydrodynamic Fluctuations, Broken Symmetry and Correlation Functions* (Benjamin, Reading, MA, 1975).
- [35] S. V. Titov, Yu. P. Kalmykov, M. A. Cherkasskii, K. D. Kazarinov, and A. S. Titov, Inertial magnetization dynamics of ferromagnetic nanoparticles near saturation, *J. Commun. Technol. Electron.* **68**(5) (2023).
- [36] D. A. Varshalovich, A. N. Moskalev, and V. K. Khersonskii, *Quantum Theory of Angular Momentum* (World Scientific, Singapore, 1998).
- [37] A. G. Gurevich and G. A. Melkov, *Magnetization Oscillations and Waves* (CRC Press, London, 1996).
- [38] E. T. Whittaker and G. N. Watson, *A Course of Modern Analysis*, 4th ed. (Cambridge University Press, Cambridge, England, 1927).
- [39] *Handbook of Mathematical Functions*, edited by M. Abramowitz and I. A. Stegun, Nat. Bur. Stand. Appl. Math. Ser. (U.S. GPO, Washington, DC, 1965), Vol. 55.
- [40] H. Hancock, *Lectures on the Theory of Elliptic Functions* (Dover, New York, 1958).
- [41] Yu. P. Kalmykov and S. V. Titov, A semiclassical theory of dielectric relaxation and absorption: Memory function approach

- to extended rotational diffusion models of molecular reorientations in fluids, *Adv. Chem. Phys.* **87**, 31 (1994).
- [42] J. M. D. Coey, *Magnetism and Magnetic Materials* (Cambridge University Press, Cambridge, England, 2010).
- [43] W. T. Coffey and Yu. P. Kalmykov, *The Langevin Equation*, 4th ed. (World Scientific, Singapore, 2017).
- [44] S. V. Titov, W. J. Dowling, Yu. P. Kalmykov, and M. Cherkasskii, Nutation spin waves in ferromagnets, *Phys. Rev. B* **105**, 214414 (2022).
- [45] Y. P. Kalmykov, Extended rotational diffusion and dielectric relaxation in a constant external electric field, *Phys. Rev. A* **45**, 7184 (1992).
- [46] S. V. Titov, Y. P. Kalmykov, and W. T. Coffey, Extended rotational diffusion and dielectric relaxation of symmetrical top molecules in a DC electric field, *J. Chem. Phys.* **118**, 209 (2003).
- [47] G. A. Korn and T. M. Korn, *Mathematical Handbook for Scientists and Engineers* (McGraw-Hill, New York, 1968).